Nuclear Quadrupole Interaction in CsF*

J. W. TRISCHKA
Columbia University, New York, New York

(Received June 4, 1948)

The electric resonance method of molecular beam spectroscopy has been used under high resolution conditions to study the rotational Stark spectrum of CsF for a single rotational state of the molecule, $J=1$. In this method polar molecules in a single rotational state and a particular state of space quantization are selected from a molecular beam by means of inhomogeneous electric fields which give the desired molecules a unique, sigmoid path in the apparatus. Changes in the beam intensity are observed when a change in the space quantization of the molecule is produced by an oscillating electric field transverse to a homogeneous, steady electric field. For weak electric fields the observed line widths agree well with the estimated uncertainty width of 10 kc/sec. At stronger fields inhomogeneities in the field cause a broadening of the lines. At sufficiently strong fields the spectrum for CsF contains several broad lines, each of which is due to transitions of molecules in a particular vibrational state. As the field strength is decreased the resolution improves and these lines reveal a complex fine structure, the principal features of which can be explained by the interaction of the electric quadrupole moment of the Cs nucleus, spin 7/2, with the molecular electrons and the F nucleus. The F nucleus, spin 1/2, has no quadrupole moment. A complete, quantitative explanation of the spectra requires the existence of a cosine type coupling between the nuclear spins and the molecular spin of the form $c\mathbf{I}\cdot\mathbf{J}$, and a correction for the spin-spin interaction of the two nuclei. At weak fields a different type of spectrum appears, permitting an independent evaluation of the nuclear-molecular interactions. The data allows a determination of both the magnitude and sign of the interaction constants. The quadrupole interaction, defined by $(e^2q'Q/2h)$, is $(+0.310\pm0.002)$ mc/sec. The constants, c/h, for the $\mathbf{I}\cdot\mathbf{J}$ interactions for F and Cs are, respectively, $(+1.6\pm2)$ kc/sec and (0 ± 1) kc/sec. The difference in the quadrupole interaction for the first two vibrational states is less than the experimental error; i.e., less than one percent. Application of the method to the measurement of various molecular constants is discussed briefly at the end of the paper.

I. INTRODUCTION

THE magnetic resonance method of molecular beam spectroscopy has been used for the measurement of the electric quadrupole moment of the deuteron[1] and the quadrupole interaction in the sodium halides.[2] A significant difference between these two experiments is that in HD and D_2 the spectra can be attributed to molecules having specific, small values of the rotational quantum number, J; whereas, in the sodium halide experiments a statistical analysis involving many $J\gg1$ is necessary to account for the spectra. This difference is a result of the large difference in the temperatures of the two molecular sources.

The advent of the electric resonance method[3] has now made possible measurements of the quadrupole interaction in molecules in a specific rotational state, even though the molecular beam is produced by a high temperature source. The essence of the method is that it selects for study only that part of the beam, about one part in ten thousand, which contains molecules in a particular J state. Its advantages for high temperature beams are the simplicity of interpretation of results and greater accuracy.

The electric resonance apparatus, shown schematically in Fig. 1,** makes use of the deflecting power of the inhomogeneous fields (A- and B-fields) to select for detection polar molecules with a particular J and a particular electric quantum number, m_J. The wire stop eliminates molecules with large values of J, as they are not appreciably deflected by the A- and B-fields. In passing through a homogeneous electric field (C-field) the molecules can change their state of space-quantization (change in m_J) through absorption or stimulated emission of radiation in the presence of a superposed oscillating electric field set at a frequency corresponding to the energy difference of the initial and final states. When this occurs they fail to reach the detector, as shown by the dashed line in Fig. 1, and the measured beam intensity drops.

* Publication assisted by the Ernest Kempton Adams Fund for Physical Research of Columbia University.

[1] J. M. B. Kellogg, I. I. Rabi, N. F. Ramsey, and J. R. Zacharias, Phys. Rev. **57**, 677 (1940).

[2] W. A. Nierenberg and N. F. Ramsey, Phys. Rev. **72**, 1075 (1947).

[3] H. K. Hughes, Phys. Rev. **72**, 614 (1947).

** The author is indebted to Dr. H. K. Hughes for the use of this figure, which is Fig. 1 in reference 3.

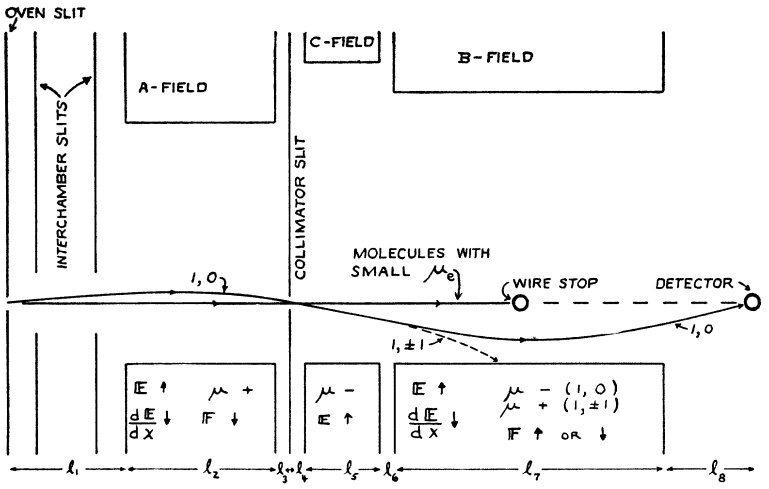

FIG. 1. Schematic diagram of electric resonance apparatus.

It has been shown[3] that the spectral lines in CsF resulting from such a change in m_J yield values of the electric dipole moment and moment of inertia of the molecules. The present paper is a report of an experimental study of these lines in CsF under high resolution conditions and an analysis of the spectra observed. With the present high resolution the single lines found by Hughes[3] show a fine structure which can be attributed to two principal causes: *viz.*, the presence in the beam of molecules in different vibrational states and the electric quadrupole moment of the Cs nucleus. Secondary details of this fine structure are explained by assuming that a cosine type coupling exists between the nuclear spins and the molecular rotation and by making a small correction arising from the magnetic dipole-dipole interaction of the Cs and F nuclei.

II. EXPERIMENTAL DETAILS

The apparatus used in these experiments is essentially the same as that used, and described in considerable detail, by Hughes,[3] with one important exception. This is the *C*-field, which is completely new.

C-Field

The component of the apparatus crucial for high resolution is the *C*-field. This must produce an electric field of great uniformity. Figure 2 shows the essential elements of the field used in these experiments. Two parallel, brass plates, $\frac{1}{4}$ inch thick, 1 and 2, are clamped together against three, ground, quartz spacers and mounted so that the molecular beam passes midway between them. Plate 2 is composed of two parts, 3 and 4, separated by a space of 0.016 inch. A steady, homogeneous electric field is produced over the length of 3 and over the height of the beam, about 5 mm, by applying a d.c. voltage from *B*-batteries to 1 and 2. Three and 4 are at the same d.c. potential. An oscillating electric field is superposed on the steady fields by connecting the output of a vacuum tube oscillator to 3 and 4. In this way the oscillating field has an appreciable strength only in the region where the steady field is uniform.

The field gap is 0.4983 cm. The overall length is 6 cm, and the length (along the beam) of 3 is 4 cm. The plates are ground flat to 0.00025 cm and gold-plated to eliminate changes in the contact potential difference from tarnishing of the brass.

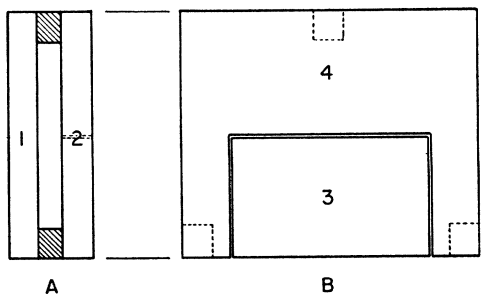

FIG. 2. Two views of the *C*-field, showing the basic features of the design. *A* is a view in the direction of the molecular beam. *B* is a side view of *A*.

Resolution

The resolution possible with the present C-field construction is determined by the uniformity of the electric field and by its effective length. The lower limit of resolution set by the non-uniformity of the field corresponds to 1 part in 2000 of the field strength or 1 part in one thousand of the frequency, since the frequency of the rotational Stark line varies as the square of the field. This gives an estimated line width (full width at half-maximum) of 7 kc/sec at a transition frequency of 3.7 mc/sec.

The width to be expected from the uncertainty relationship

$$\Delta\nu\Delta\tau\sim 1 \qquad (1)$$

is 10 kc/sec. $h\Delta\nu$ is the uncertainty in the energy and $\Delta\tau$ is the time spent by the molecules in the radiation field. In this case $\Delta\tau$ is computed using the most probable velocity of the molecules at an oven temperature of 800°K, 4×10^4 cm/sec, and an effective length of the field of 4 cm.

The effect of the magnitude of the oscillating field on the resolution can be calculated from the expression for the transition probability[3]

$$P=0.5/[1+(E_{dc}/E_{rms})^2(1-f/f_0)^2]. \qquad (2)$$

E_{rms} is the rms value of the oscillating field, while E_{dc} is the value of the steady field. For experiments with strong fields, where this formula is valid, typical values were $E_{dc}=100$ v/cm and $E_{rms}=0.16$ v/cm; $f_0=3.7$ mc/sec. These give a width of 12 kc/sec.

The theoretical width resulting from a combination of the above estimates was not calculated. However, the observed width of lines produced by a single transition in the vicinity of 3.7 mc/sec was 16 kc/sec, so that it is reasonable to conclude that the experimental limit of resolution was reached.

The line width at weak fields, $E_{dc}\sim 2$ v/cm, is in close agreement with the width calculated from (1). E_{rms} was 1 v/cm.

Beam Intensities

The CsF beam was detected with a hot W wire, 0.005 inch in diameter, at the surface of which the neutral molecules were ionized. The ion current was measured with a d.c. amplifier[4] employing an FP54 tube and a 5×10^{10} ohm grid resistor. The sensitivity of the amplifier was 50,000 mm/volt on a scale two meters from the galvanometer.

The total beam, with the stop-wire removed, gave an equivalent galvanometer deflection of 300,000 cm. The refocused beam in the (1,0) state produced a 30 to 40 cm deflection. The need for such a large beam arose from the fact that a great many lines are resolved; in fact the maximum change in beam strength corresponding to a single transition gave a deflection of only 2 to 3 cm.

Three factors contributed to the galvanometer deflection at any instant of time: (1) detector "noise", (2) a residual beam; i.e., a beam detected with the wire-stop in place, but with the A- and B-fields turned off, (3) the refocused beam. The residual beam was usually as large as, sometimes less than, the refocused beam. Unsteadiness in all of these factors, chiefly the detector "noise", required that measurements be made by noting the change in deflection produced by turning the oscillator on and off and averaging four successive readings. With this procedure the minimum detectable change in beam strength was 3 mm, under the best conditions. This corresponds to a change of about 10^4 molecules/sec or 10^6 molecules/cm^2/sec for a beam 5 mm high.

Procedure

The procedure for measuring changes in beam strength has been detailed above. In addition, measurements were made of the frequency of the oscillating field and the voltage applied to the homogeneous field. At strong fields the relative positions of the lines in the fine structure due to the nuclear-molecular interactions is independent of the field strength. Hence, it is possible to fix the frequency and vary the field, to scan the spectrum, or to fix the field and vary the frequency. The latter method was used in gathering all the important data reported on here. The voltage was measured with a type K potentiometer and held constant to 1 part in 5000. Frequency was measured with a General Radio Type 624A heterodyne frequency meter to 1 part in 10,000.

[4] D. B. Pennick, Rev. Sci. Inst. 6, 115 (1935).

Measurements at zero electric field would have been desirable both because of the simplicity of the line structure and as an independent check on the strong field measurements. However, the transition probability vanishes at zero field.[3] Thus it was necessary to work at a field strong enough so that transitions could be observed but not so strong that effects caused by the interaction of the molecule with the field were large.

In practice it was found that as the strength of the homogeneous field was decreased the strength of the refocused beam dropped because some of the molecules were undergoing nonadiabatic transitions[5] in the regions between the C-field and the two focusing fields. This effect set the lower limit of weak field operation.

III. THEORY

The Hamiltonian used as a basis for theoretical calculations was

$$\begin{aligned}\mathcal{H}=&(h^2/2A)\mathbf{J}^2-\boldsymbol{\mu}\cdot\mathbf{E}\\&-e^2q'Q/I_1(2I_1-1)(2J-1)(2J+3)\\&\times[3(\mathbf{I}_1\cdot\mathbf{J})^2+\tfrac{3}{2}(\mathbf{I}_1\cdot\mathbf{J})\\&-I_1(I_1+1)J(J+1)]+c_1\mathbf{I}_1\cdot\mathbf{J}\\&+c_2\mathbf{I}_2\cdot\mathbf{J}+g_1g_2\mu_N{}^2/r^3(2J+3)(2J-1)\\&\times[3(\mathbf{I}_1\cdot\mathbf{J})(\mathbf{I}_2\cdot\mathbf{J})+3(\mathbf{I}_2\cdot\mathbf{J})(\mathbf{I}_1\cdot\mathbf{J})\\&-2\mathbf{I}_1\cdot\mathbf{I}_2J(J+1)]. \quad (3)\end{aligned}$$

The first term, in which A is the moment of inertia of the molecule and J is the rotational quantum number, corresponds to the mechanical energy of rotation of the molecule. This remains unchanged in these experiments, since $J=1$ at all times. The second term gives the splitting produced by the interaction between the electric dipole moment, μ, and the electric field, E. Reference 3 gives a summary of the energy levels arising from this term alone. The third term is the operator for the interaction between the electric quadrupole moment of the Cs nucleus, Q, and the electric field gradient at this nucleus produced by the remaining charges in the molecule. Q and q' are defined by Nordsieck[6] and in reference 1. I_1 is the spin of the Cs nucleus. The theory of Fano[7] was used in calculating the matrix elements given by this term. Since the F spin is $\frac{1}{2}$, this nucleus has no electric quadrupole moment, whence the absence of a quadrupole term for it in (3). The third and fourth terms, where I_2 is the spin of the F nucleus, represent perturbations produced by a cosine coupling between the nuclear spins and the molecular rotation. They can be thought of as representing the interaction between the nuclear magnetic dipole moment and a magnetic field produced at the nucleus by a current set up by the molecular electrons as a result of the rotation of the molecule. A more detailed picture of this type of interaction is discussed by Foley[8] and by Wick.[9] Calculations for this interaction made use of the formulas presented by Nierenberg and Slotnick.[10] The last term comes from the small perturbation produced by the coupling of the two nuclear magnetic dipole moments. g_1 and g_2 are the nuclear gyromagnetic ratios of the Cs and F nuclei respectively; μ_N is the nuclear magneton and r is the internuclear distance of the molecule. The operator in this form is taken from reference 1. The matrix elements, calculated by Nierenberg,[11] are given in an appendix to this paper.

In analyzing the observed spectra it is necessary to take into account the fact that the refocused beam contains molecules in several different vibrational states. It is reasonable to assume that the main effect of vibration is to change the average electric dipole moment and the average moment of inertia of the molecule as the vibrational state changes. This means that the second term in (3) will be different for different vibrational states, and the observed spectrum will be a superposition of lines from molecules in different vibrational states. No theoretical estimates are available for the effect of vibration on the constants in the other terms of (3). However, from the data presented in this report it is possible to make an experimental estimate of the magnitude of such an effect.

In general the terms in (3) will be different for different isotopic species. However, CsF has only one isotopic species. This greatly simplified the experimental work and the analysis of the data.

In the application of the perturbation theory

[5] I. I. Rabi, Phys. Rev. **49**, 324 (1936).
[6] A. Nordsieck, Phys. Rev. **58**, 310 (1940).
[7] U. Fano, J. Res. Nat. Bur. Stand., Wash., **40**, 215 (1948). Energy level charts in this paper are directly applicable to CsF.
[8] H. Foley, Phys. Rev. **72**, 504 (1947).
[9] G. C. Wick, Phys. Rev. **73**, 51 (1948).
[10] W. A. Nierenberg and M. Slotnick, Phys. Rev. **73**, 1437 (1948).
[11] W. A. Nierenberg, private communication.

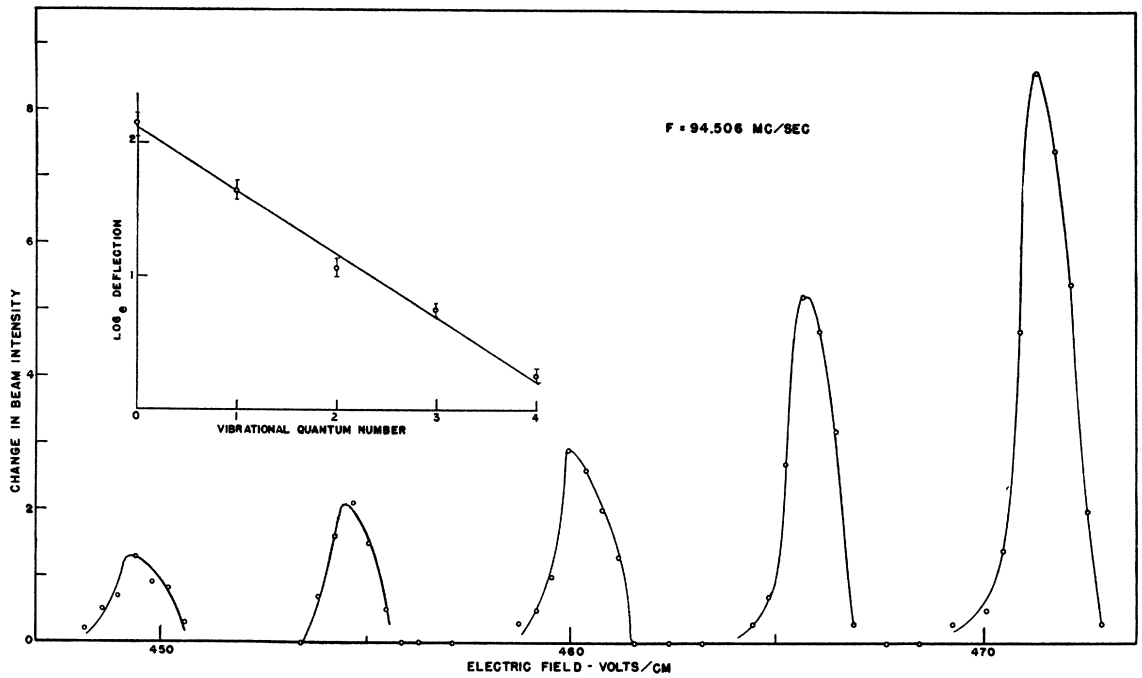

FIG. 3. Spectrum at strong fields, showing lines produced by molecules in five different vibrational states. The fine structure resulting from nuclear-molecular interactions is not resolved. The graph in the upper left corner is a semi-log plot showing the distribution of vibrational states. v is the vibrational quantum number.

to computing the characteristic values of (3) it is convenient to distinguish two cases for which the theory is relatively simple. "Strong fields" are defined for this purpose as fields for which

$$e^2q'Q \ll \mu^2E^2/\hbar^2/2A \ll \hbar^2/2A \times J(J+1). \quad (4)$$

In this case the electrical terms are diagonal in an m_J, m_{I_1} representation, i.e., the molecular and nuclear spins are effectively decoupled. It is noteworthy that in this instance, $\hbar^2/2A \times J(J+1) \gg \mu^2E^2/\hbar^2/2A$, there is a negligible mixing of J-states and therefore Casimir's expression for the quadrupole interaction, which is diagonal in J, is correctly applied. Hence, since I and J are in effect decoupled, the matrix elements in reference 1 are suitable. For CsF the errors in making this approximation are less than the errors of measurement, for $e^2q'Q/2h \sim 0.3$ mc/sec while $(\hbar^2/2Ah)J(J+1) \sim 10{,}000$ mc/sec.

An important consequence of the strong field theory is that the fine structure produced by the terms beyond the second one in (3) is independent of the value of the field, thus rendering unnecessary a knowledge of the magnitude of the field.

"Weak fields" are defined by

$$e^2q'Q \gg \mu^2E^2/\hbar^2/2A. \quad (5)$$

In this case I_1 and J are strongly coupled and an F_1, m_{F_1} representation is used, so that the quadrupole interaction will contribute only diagonal elements to the energy matrix. $\mathbf{F}_1 = \mathbf{I}_1 + \mathbf{J}$.

IV. ANALYSIS OF SPECTRA

Value of J

It was decided at the beginning of these experiments to obtain spectra from molecules for which $J=1$, this being the state easiest to refocus with the present apparatus. However, it is possible to refocus CsF molecules with several values of $J \geqslant 1$, depending on the A- and B-field voltages. In addition, more than one value of J may be represented in the beam refocused for a particular set of refocusing conditions. Two different methods were used for determining J.

The first method makes use of the uniqueness of the fine structure for a given $(J, m_J) \rightarrow (J, m_J')$ transition. This was not so easy as might be anticipated. For example, calculations showed

that the $(2, \pm 1) \rightarrow (2, \pm 2)$ and $(1,0) \rightarrow (1, \pm 1)$ transitions should give fine structure patterns which are identical at strong fields, except for a difference in sign, and small differences due to the $\mathbf{I} \cdot \mathbf{J}$ interaction not experimentally detectable. At weak fields the predicted patterns are different, but still not sufficiently different to make a distinction experimentally. However, when the value of the quadrupole interaction computed from the weak field data was compared with the value computed from the strong field data it was found that the two values disagreed by much more than the experimental error if the spectra were attributed to $J=2$. On the other hand, they agreed satisfactorily when the assumption was made that $J=1$.

In the second method observations of the $\boldsymbol{\mu} \cdot \mathbf{E}$ interaction were made for two different values of J and compared. Such a comparison permits an unambiguous identification of both J's. A brief review of the procedure follows.

The transition frequency corresponding to $(J, m_J) \rightarrow (J, m_J')$ is given by[3]

$$\nu = K_1(J, m_J, m_J')E^2 + K_2(J, m_J, m_J')E^4, \quad (6)$$

if only the $\boldsymbol{\mu} \cdot \mathbf{E}$ interaction is taken into account. This frequency can be readily calculated once the analysis of the fine structure produced by the other terms in (3) has been carried out.

The most precise way of comparing results for two different values of J is to obtain the ratio

$$K_1(J_1, m_J, m_J')/K_1(J_2, m_J'', m_J'''), \quad (7)$$

which can be predicted from the theory. K_1 was determined with a precision of 1 part in 3000 by plotting ν/E^2 *vs* E^2 and extrapolating the straight line so obtained to $E=0$. In this way the transitions $(1, 0) \rightarrow (1, \pm 1)$ and $(2, 0) \rightarrow (2, \pm 1)$ were identified. An additional check on the $(1, 0) \rightarrow (1, \pm 1)$ transition was also obtained by a comparison with Hughes'[3] results.

The spectra analyzed in this paper are all from molecules for which $J=1$. The spectra obtained for $J=2$ were observed at fields too high for good resolution, and were consequently of no value in evaluating the nuclear-molecular interactions.

Vibrational Effects

Figure 3 shows the spectrum obtained with an electric field so strong that the $(1, 0) \rightarrow (1, \pm 1)$ transitions are displayed for molecules in the first five vibrational states. In this run the fre-

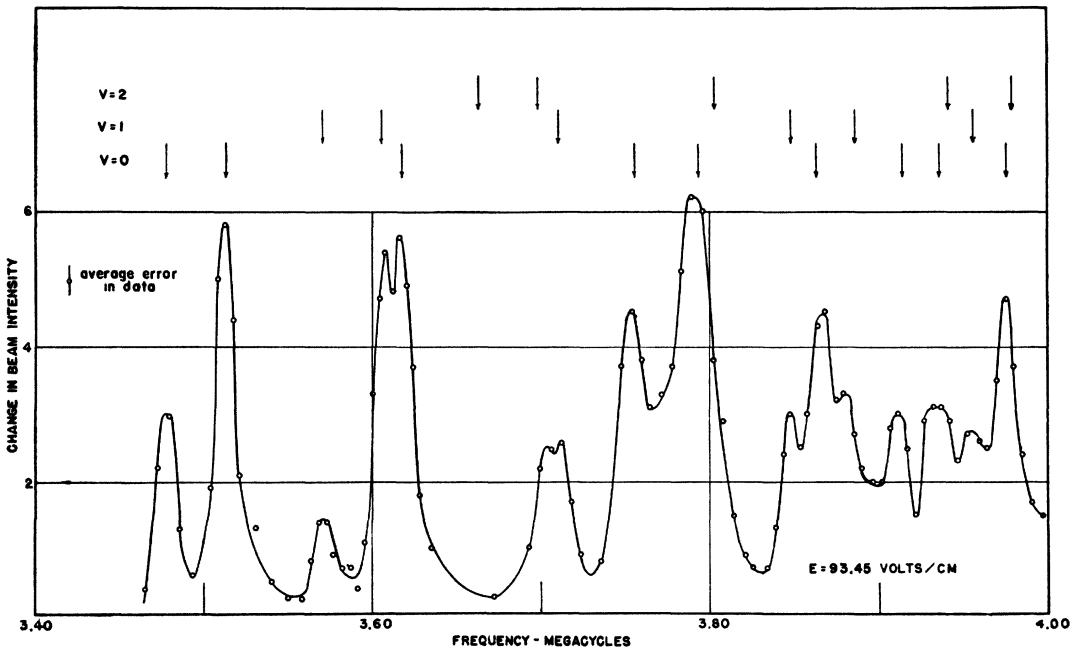

FIG. 4. Strong field spectrum showing the fine structure produced by the nuclear-molecular interactions for molecules in several vibrational states. Arrows at the top of the figure indicate theoretical line positions. v is the vibrational quantum number.

quency was held constant at 94.506 mc/sec and the field varied. That this spectrum does show the presence of several vibrational states can be demonstrated in two ways: (1) When spectra were observed at several different field strengths, a straight line resulted from a plot of ν/E^2 *vs* E^2 for each of the spectral lines. This would be expected from (6) if the individual lines arise from molecules having slightly different values of μ and A; (2) a plot of the logarithm of the peak intensities of the lines as a function of the vibrational quantum number, v, is a straight line (shown in the upper left hand corner of Fig. 3). Thus the distribution of the molecules producing the lines is the same as the distribution of vibrational states in a molecular gas.

Data was taken at larger fields than those shown in Fig. 3 to insure that the most intense line in the figure actually corresponded to $v=0$.

The width of the lines in Fig. 3 is produced by the unresolved fine structure, arising from the nuclear-molecular interactions and the field inhomogeneity. The latter alone would produce a line width of 0.5 v/cm.

Since the frequency separations of the "vibration" lines varies as E^2 while the fine structure produced by the nuclear-molecular interactions remains constant until intermediate fields are reached, it is evident that the spectra from the molecules in different vibrational states will eventually overlap as the field strength is decreased. This is the case for the results shown in Fig. 4 where the lines corresponding to various vibrational states are indicated by the arrows at the top of the figure for three different states. It is clear from the complexity of the spectra in Fig. 4 that the data presented in Fig. 3, where the vibrational effect is completely unambiguous, is invaluable in assigning the lines in Fig. 4 to molecules in the various vibrational states.

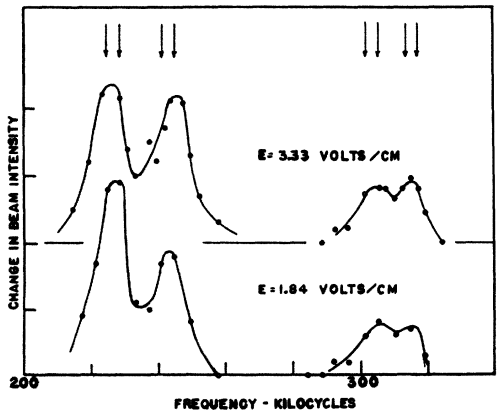

FIG. 5. Weak field spectra for two different values of the field. Arrows show the theoretical positions of lines at zero field.

For the weak fields indicated in Fig. 5 the spectral shift produced by the $\boldsymbol{\mu}\cdot\mathbf{E}$ interaction for molecules in different vibrational states is less than 1 kc. This is far below the resolution of the apparatus.

Structure At Strong Fields

Figure 4 shows the spectrum obtained at strong fields, but with sufficient resolution to reveal the fine structure produced by the nuclear-molecular interactions. Since the main features of this structure are due to the quadrupole interaction it is necessary to make certain that the "strong field" theory applies. Discussion, at this point, will center on the lines for which $v=0$. There are nine such lines, as indicated by the arrows in the figure. The total spread of the spectrum is a rough measure of the quadrupole interaction. This is 0.499 mc/sec. The frequency corresponding to the $\boldsymbol{\mu}\cdot\mathbf{E}$ interaction alone is 3.74 mc/sec, so that the ratio of the two is 7.5/1. Calculations show that this ratio is large enough to satisfy (4) very well.

The detailed calculations of the theoretical line positions are too lengthy to present here. Therefore, only pertinent aspects of the theory will be given. Since $I_1=7/2$, $I_2=1/2$ and $J=1$, at most 48 energy levels will be involved. The quadrupole interaction alone gives rise to 24 energy levels which are degenerate in such a way that 8 levels correspond to $m_J=\pm 1$ and 4 to $m_J=0$. If the oscillating field is perpendicular to the steady field the selection rules are $\Delta m_J=\pm 1$ and $\Delta m_{I_1}=0$, so that 14 lines are predicted. Of these, only 8 should be resolved. Since the oscillating field actually has components both parallel and perpendicular to the steady field, there is a small possibility of observing lines for which $\Delta m=0$, $(m=m_J+m_{I_1})$. No such lines were found, however.[12]

[12] The presence of corresponding lines was observed at intermediate fields. Results at these fields are not presented because the theoretical calculations are highly involved, and preliminary calculations showed that no new information was available from these measurements.

An examination of Fig. 4 reveals nine lines instead of eight. A detailed comparison of the experimental and theoretical lines gives good agreement for all of the lines except lines 7 and 8, counting from low to high frequencies. In this case the predicted line falls midway between 7 and 8. Hence, we conclude that the results cannot be explained by the quadrupole interaction alone, but the contributions of the other terms in (3) must be considered.

Calculations for the $\mathbf{I}\cdot\mathbf{J}$ interaction show that the effect of the Cs spin is to shift the quadrupole lines slightly, while the F spin produces a splitting of the levels for $m_J=\pm 1$. Because of the way in which some of the states for $m_J=\pm 1$ are mixed by the quadrupole interaction the effect of the $\mathbf{I}\cdot\mathbf{J}$ interaction for the F nucleus, is largely suppressed except for one of the quadrupole levels. It is precisely the transitions from this split level which correspond to lines 7 and 8. The theory shows that the constant c_2 is just equal to the energy separation of lines 7 and 8. As the result of several runs this separation is found to be 22 kc/sec. However, this must be corrected for the effect of the nuclear dipole-dipole interaction.

Calculations for the dipole-dipole interaction show that its observable effects in this case are indistinguishable from the effect of the $\mathbf{I}\cdot\mathbf{J}$ interaction. Fortunately the values of g_1, g_2 and r are known so that exact calculations can be made. The result is a correction of 4 kc/sec which makes the value of $c_2/h=18$ kc/sec.

An additional comparison between theory and experiment can be made by considering the line intensities. For example, the ratio of the intensities of lines 1 and 2 should be one to two according to the theory, and this agrees with the intensities shown in Fig. 4. Agreement also exists for line 3, theoretical weight two, on this scale. Lines 4 and 5 are made up of a number of unresolved lines, but the observed intensities seem to be in agreement with estimates made by combining the effects of the theoretical lines. Lines 6 and 9 should each have a weight of one, and their large, observed peak intensities are doubtless the result of the presence of so many nearby lines for $v=0$ and $v>0$. Intensity considerations also give striking confirmation of the predictions for the $\mathbf{I}\cdot\mathbf{J}$ interaction. The line predicted between 7 and 8, considering the quadrupole coupling alone, had a weight of one. Lines 7 and 8 are clearly much weaker than 6 and 9.

TABLE I. Comparison of experimental and theoretical relative positions of lines at strong fields for $v=0$. Frequencies in kc/sec. Lines counted from the low frequency end of the spectrum. (Cf. Fig. 4.)

Line	Exp.	Theor.
1	−263	−263
2	−228	−228
3	—	−123
4	+ 14	+ 15
5	+ 51	+ 53
6	+126	+123
7	+172	+174
8	+195	+196
9	+236	+236

The effect of vibration on the quadrupole interaction must be less than one percent for CsF, since the fine structure separations for higher vibrational states is in experimental agreement with the separations for $v=0$. The absence of line 1 for $v=2$ in Fig. 4 is due to the absence of data in this run. Other runs show the line to be present. Additional lines for $v>0$ beyond the high frequency end of Fig. 4 have also been observed and their positions agree with the theoretical predictions.

Structure at Weak Fields

Figure 5 shows the spectra obtained at two different, weak electric fields. According to the theory for the quadrupole interaction at weak fields there will be three levels corresponding to $F_1=9/2,\ 7/2,\ 5/2$. Thus two lines are predicted from $\Delta F_1=\pm 1$. Figure 5, however, shows two groups of lines, a pair of lines in the low frequency group and a broad line, presumably made up of several unresolved lines, at a higher frequency. If the $\mathbf{I}\cdot\mathbf{J}$ interaction is taken into account, this discrepancy is resolved. The theory predicts four lines, occurring in two closely spaced pairs in the low frequency group, and four lines nearly evenly spaced in the high frequency group. These lines are indicated by the arrows in Fig. 5. As was the case at strong fields the dipole-dipole interaction is indistinguishable from the $\mathbf{I}\cdot\mathbf{J}$ interaction experimentally. Again, a small correction must be made for it.

Although the effect of the $\boldsymbol{\mu}\cdot\mathbf{E}$ interaction is small in comparison with the quadrupole effect it is not entirely negligible for the fields indicated

TABLE II. Experimental positions of lines at weak fields. Frequencies are in kc/sec. Lines are counted from the low frequency end of the spectrum. (Cf. Fig. 5.)

Line	ν
1	226
2	243
3	310

in Fig. 5. Calculations using the appropriate formula in reference 10 show that only the level $F_1=5/2$ is measurably affected. The result is that there should be 14 unresolved lines in the high frequency group. Since the positions of these lines depend on field strength the experimental agreement at the two field values shown in Fig. 5 seems strange. However, the lines shift in relative positions with no appreciable change in their center of gravity in going from the smaller to the larger field.

No effort has been made in this case to calculate the relative intensities of the lines.

The complete explanation of these results by the analysis outlined above leaves no room for effects due to vibration of the molecules. The experimental upper limit set on the possible change of the quadrupole interaction with vibrational state is about 2 percent. Thus, the strong field data are more conclusive on this point than the weak field data.

V. RESULTS

Table I shows the experimental and theoretical positions of the lines in Fig. 4 for $v=0$. The center of reference is the frequency which would correspond to the $\mu\cdot\mathbf{E}$ transitions alone. In this table theoretical lines which would be experimentally unresolved have been "merged" in calculating the theoretical positions presented. Table II shows the experimental positions of the lines in Fig. 5. Table III shows the constants required to give the best fit between the theory and the experimental results. The magnetic fields at the Cs and F nuclei, H_1 and H_2, produced by the molecular rotation are computed from c_1 and c_2 by means of the formula

$$H=(hc/\mu_N g). \tag{8}$$

This is the field per unit rotation.

TABLE III. Interaction constants calculated from the strong and weak field spectra. Subscripts 1 and 2 refer to Cs and F nuclei respectively. See text for definitions of symbols.

Quantity	Strong field	Weak field	Average
$e^2qQ/2h$, mc/sec	+0.312±0.002	+0.307±0.004	+0.310±0.002
c_1/h, kc/sec	−0.6±1	+0.5±1	0±1
c_2/h, kc/sec	+18±2	+14±3	+16±2
H_1, gauss	−1±2	+1±2	0±2
H_2, gauss	+4.6±0.5	+3.5±0.7	+4.0±0.5

The errors stated are a result of uncertainty in estimating line positions. The value of the quadrupole interaction constant at strong electric fields is based on the positions of all of the observed lines and is more accurate than the value determined at weak fields, where the error in determining the center of the line pattern for the high frequency group was relatively large.

It is important to note the relative merits of evaluating the constants in Table III from strong and weak field data. Besides the relative accuracies discussed above there are features unique to each case. The sign of the quadrupole interaction constant can be determined from the strong field data by observing the asymmetry of the fine structure pattern. The weak field data yields only the magnitude and not the sign of this constant. On the other hand the sign of c_2 can be determined only from the weak field data and not from the strong field data. c_1 is so small that its sign is in doubt in either case in these experiments, but theoretically the sign could be determined from either the strong or weak field results.

VI. DISCUSSION

It is of interest to compare the results presented here with results obtained by the magnetic resonance method. To make this comparison for the quadrupole interaction, unpublished data of Millman and Kusch on the Cs resonance in CsF was used. The theoretical shape for their resonance curve is given by Feld and Lamb in Fig. 6 of their paper.[13] This curve has a central maximum with six symmetrically placed "spikes" of decreasing intensity on either side of it. The experimental curve is a perfectly smooth, resonance curve, the "spikes" being unresolved. It is therefore difficult to make an accurate estimate of the quadrupole interaction constant without a detailed analysis of the resolution of the magnetic resonance apparatus. In lieu of this the half width of the experimental curve was taken arbitrarily to

[13] B. T. Feld and W. E. Lamb, Phys. Rev. 67, 15 (1945).

be the same as the distance between $1-2x$ and $1+2x$ on the theoretical curve. The result,

$$e^2q'Q/2h=0.31 \text{ mc/sec}$$

agrees even better than might be expected, considering the approximations made in the analysis, with the result reported here. The sign of the interaction cannot be determined from the magnetic resonance data.

It was not thought worth while to attempt an estimate of the constant c_1/h for the Cs $\mathbf{I}\cdot\mathbf{J}$ interaction from the magnetic resonance data, since the accuracy of such an estimate would be at least an order of magnitude less than the accuracy of this constant determined by the electric resonance method. However, the agreement between the two values of $e^2q'Q/2h$ indicates that the small value of c_1/h reported in this paper is consistent with the magnetic resonance results.

The value of H_2 presented in Table III can be compared with the value calculated by Wick[9] using the magnetic resonance data from reference 2; *viz.*, 1.8 gauss. The discrepancy between the two values, amounting to more than a factor of two, is far beyond the experimental error in both methods of measurement. If this discrepancy is real, it may indicate that the $\mathbf{I}\cdot\mathbf{J}$ interaction is given by $f(J)(\mathbf{I}\cdot\mathbf{J})$ instead of $c\mathbf{I}\cdot\mathbf{J}$, where $f(J)\rightarrow 1$ for $J\gg 1$. Further experiments are indicated in which the $\mathbf{I}\cdot\mathbf{J}$ interaction is studied as a function of J. It is important to note that the sign of the interaction is not given by the magnetic resonance method.

Since the measurements of the quadrupole interaction give neither the value of q' nor of Q, but only their product, the important problem of separating the two quantities still remains. However, if the same nucleus is present in different molecules, the product, $q'Q$, gives some information about the changes in molecular binding. In this connection it is interesting to note the striking difference between the present results and those deduced from measurements made by the magnetic resonance method on Cs_2;[14] *viz.*,

$$e^2q'Q/2h=0.074 \text{ mc/sec}$$

This difference is qualitatively the same as that already noted by Nierenberg and Ramsey[2] for the sodium halides and Na_2. The theory used as a basis for the above estimate for Cs_2 has been developed by Foley.[15]

This paper has been directed at understanding the nuclear-molecular interactions revealed in the fine structure observed in transitions of the type $(J, m_J)\rightarrow(J, m_J')$. However, with the present high resolution, valuable information about certain molecular constants can be obtained. In the first place, the electric dipole moment and moment of inertia of the molecule can be re-evaluated with greater accuracy than was possible before.[3] Secondly, the variation of the product, μ^2A, with vibrational quantum number can be found and should yield some information about the shape of the potential energy curve for the molecule, especially if either μ or A can be determined separately with high accuracy. Thirdly, the slope of the straight line in the upper left corner of Fig. 3 gives the vibrational constant ω_e, although not with great accuracy, perhaps 10 percent in this instance, because of the large uncertainty in the source temperature.[16]

The author wishes to thank Professor I. I. Rabi for suggesting this research and for many helpful discussions. He also wishes to thank Mr. L. Grabner and Mr. S. Jacobson for their help in the laboratory. The help of Mr. M. Slotnick and Dr. W. A. Nierenberg in the theoretical work is gratefully acknowledged.

APPENDIX

The first order energy terms for the magnetic dipole-dipole interaction under weak field conditions are[11]

$$g_1g_2\mu_N^2/r^3(2J+3)(2J-1)\times[3g_J\{F_1(F_1+1)-I_1(I_1+1)-J(J+1)\}+2g_{I_1}J(J+1)]\mathbf{I}_2\cdot\mathbf{F}, \quad (9)$$

where

$$g_J=[F_1(F_1+1)+J(J+1)-I_1(I_1+1)]/2F_1(F_1+1), \quad (10)$$

$$g_{I_1}=[F_1(F_1+1)+I_1(I_1+1)-J(J+1)]/2F_1(F_1+1), \quad (11)$$

$$\mathbf{I}_2\cdot\mathbf{F}=1/2\times[F(F+1)-F_1(F_1+1)-I_2(I_2+1)], \quad (12)$$

$$\mathbf{F}_1=\mathbf{I}_1+\mathbf{J}, \ (F_1=I_1+J, I_1+J-1, \cdots|I_1-J|), \quad (13) \text{ and}$$

$$\mathbf{F}=\mathbf{F}_1+\mathbf{I}_2, \ (F=F_1+I_2, F_1+I_2-1, \cdots|F_1-I_2|). \quad (14)$$

The other symbols are defined in the text.

For strong electric fields the first order energy terms for this interaction are

$$2g_1g_2\mu_N^2/r^3(2J+3)(2J-1)\times[3m_J^2-J(J+1)]m_{I_1}m_{I_2}, \quad (15)$$

where

$$m_J=J, J-1, \cdots -J, \quad (16)$$

$$m_{I_1}=I_1, I_1-1, \cdots -I_1, \text{ and} \quad (17)$$

$$m_{I_2}=I_2, I_2-1, \cdots -I_2. \quad (18)$$

[14] P. Kusch, S. S. Millman, and I. I. Rabi, Phys. Rev. **55**, 1176 (1939).

[15] H. M. Foley, Phys. Rev. **71**, 747 (1947).

[16] The value of ω_e obtained from Fig. 3 is 270 ± 30 cm^{-1}. The oven temperature was 800°K.